

Original Research

# Global RNA Interaction and Transcriptome Profiles Demonstrate the Potential Anti-Oncogenic Targets and Pathways of RBM6 in HeLa Cells

Ping Peng<sup>1</sup>, Qingqing Yin<sup>2,§</sup>, Wei Sun<sup>1</sup>, Jing Han<sup>1</sup>, Hao Guo<sup>2</sup>, Chao Cheng<sup>3,§</sup>, Dongbo Liu<sup>1,\*</sup>

Academic Editor: Roberto Bei

Submitted: 22 March 2024 Revised: 1 June 2024 Accepted: 11 June 2024 Published: 23 September 2024

#### Abstract

Background: The fate and functions of RNAs are coordinately regulated by RNA-binding proteins (RBPs), which are often dysregulated in various cancers. Known as a splicing regulator, RNA-binding motif protein 6 (RBM6) harbors tumor-suppressor activity in many cancers; however, there is a lack of research on the molecular targets and regulatory mechanisms of RBM6. Methods: In this study, we constructed an RBM6 knock-down (shRBM6) model in the HeLa cell line to investigate its functions and molecular targets. Then we applied improved RNA immunoprecipitation coupled with sequencing (iRIP-seq) and whole transcriptome sequencing approaches to investigate the potential role and RNA targets of RBM6. Results: Using The Cancer Genome Atlas dataset, we found that higher expression of RBM6 is associated with a better prognosis in many cancer types. In addition, we found that RBM6 knockdown promoted cell proliferation and inhibited apoptosis, demonstrating that RBM6 may act as an anti-oncogenic protein in cancer cells. RBM6 can regulate the alternative splicing (AS) of genes involved in DNA damage response, proliferation, and apoptosis-associated pathways. Meanwhile, RBM6 knockdown activated type I interferon signaling pathways and inhibited the expression of genes involved in the cell cycle, cellular responses to DNA damage, and DNA repair pathways. The differentially expressed genes (DEGs) by shRBM6 and their involved pathways were likely regulated by the transcription factors undergoing aberrant AS by RBM6 knockdown. For iRIP-seq analysis, we found that RBM6 could interact with a large number of mRNAs, with a tendency for binding motifs GGCGAUG and CUCU. RBM6 bound to the mRNA of cell proliferation- and apoptosis-associated genes with dysregulated AS after RBM6 knockdown. Conclusions: In summary, our study highlights the important role of RBM6, as well as the downstream targets and regulated pathways, suggesting the potential regulatory mechanisms of RBM6 in the development of cancer.

Keywords: RBM6; RNA interaction; DNA damage response; type I interferon; alternative splicing

#### 1. Introduction

The oncogenesis and development of cancers are very complex processes that are regulated at different molecular layers and by multiple kinds of molecules, including RNAs [1] and RNA binding proteins (RBPs) [2,3]. RBPs can interact with RNAs and influence all of the biological processes of RNAs from generation to degradation, and are often misexpressed in various cancers leading to functional consequences [4–8]. A previous study showed that 15 RBPs significantly influenced the prognostic results of patients with head and neck squamous cell carcinoma (HN-SCC) [9]. RBM3, one RNA-binding motif protein, can reduce cell apoptosis and promote the radio resistance of nasopharyngeal carcinoma by affecting the phosphoinositide 3-kinase (PI3K)/protein kinase B (AKT)/B-cell lymphoma-2 (Bcl-2) signaling pathway [10]. Moreover, RBPs are dysregulated in various cancers, leading to dysfunctional gene splicing and tumor-specific dependencies [11]. For example, it has been shown that RNA Binding Fox-1 Homolog 2 (RBFOX2)-regulated alternative splicing genes are enriched Ras Homolog Family (RHO) GTPase pathways, through which RBFOX2 reduces the metastatic potential of pancreatic ductal adenocarcinoma cells [12]. However, there has been a lack of research on the role of RBPs in cancer, especially the regulatory mechanism of splicing factors in post-transcriptional processes.

RBM6, a canonical alternative splicing (AS) factor, is frequently mutated in human cancers [13–15]. RBM6 contains several domains that are associated with AS regulation, including two RNA recognition motifs [16–19]. RBM6 is often localized in the nucleus and forms foci corresponding to splicing speckles [20]. RBM6 can regulate gene expression and AS, which are involved in tumorigenesis [21]. As a tumor-suppressor, RBM6 inhibits the growth and progression of laryngocarcinoma [22]. In hepatocellular carcinoma (HCC), RBM6 can promote cell apoptosis, and inhibit proliferation, migration, and invasion, thereby inhibiting the progression of HCC [23]. A previous study

<sup>&</sup>lt;sup>1</sup>Cancer Center, Tongji Hospital, Tongji Medical College, Huazhong University of Science and Technology, 430030 Wuhan, Hubei, China

<sup>&</sup>lt;sup>2</sup>Center for Genome Analysis, Wuhan Ruixing Biotechnology Co., Ltd., 430075 Wuhan, Hubei, China

<sup>&</sup>lt;sup>3</sup>Center for BioBigData Analysis, ABLife BioBigData Institute, 430075 Wuhan, Hubei, China

<sup>\*</sup>Correspondence: dbliu@tjh.tjmu.edu.cn (Dongbo Liu)

<sup>§</sup> Present address: Wuhan Bio-salt technology Co., Ltd., 430075 Wuhan, Hubei, China.

reported that RBM6 negatively regulates the proliferative capacity of cancer cells by displaying positional effects on AS regulation with the cooperation of RBM5 and RBM10 [24]. These findings demonstrate that RBM6 has important functions in human tumorigenesis. Thus, it is worthwhile to further study the regulatory functions of RBM6 in tumors and its downstream targets to identify novel potential therapeutic targets.

To this end, in the current study, we assessed the expression patterns and survival effects of RBM6 on 24 cancer types available in The Cancer Genome Atlas (TCGA) database. The results revealed that patients with higher RBM6 expression levels often had better overall survival in most cancer types. To further investigate how RBM6 regulates gene transcription and AS, and how RBM6 is involved in cancer progression, we constructed an RBM6 knockdown model in the HeLa cell line. Furthermore, we used RNA-seq to study global transcriptome profile in order to investigate the downstream RNA targets of RBM6 in HeLa cells and analyze the alterations of signaling pathways caused by RBM6 knockdown. We also identified the RBM6-regulated AS events (RASEs). Moreover, we identified the genes bound by RBM6 using the improved RNA immunoprecipitation and sequencing approach (iRIP-seq). The results of this study highlight the important regulatory roles and downstream targets, as well as the potential regulatory mechanisms of RBM6 in the pathogenesis or progression of tumors.

#### 2. Materials and Methods

### 2.1 Expression and Survival Pan-Cancer Analysis of RBM6 by TCGA Dataset

We downloaded and obtained the gene expression (RNA-seq) and survival information datasets of 24 cancer types from TCGA project, including tumor and normal samples, from the UCSC XENA database (https://xenabrowser.net/datapages/). Then we analyzed the expression levels of *RBM6*. The survival package in R (version 4.2.3) was used to perform survival modeling and Kaplan-Meier (KM) analyses.

#### 2.2 RBM6 Short Hairpin RNA Plasmid Construction

The short hairpin RNA (shRNA) duplexes of RBM6 were purchased from GenePharma (Suzhou, China). The negative control shRNA (shNC) sequence was: 5'-TTCTCCGAACGTGTCACGT-3' (sense), whereas the shRNA targeting *RBM6* (shRBM6) sequence was: 5'-TTCAGGTTCCTTATCAGCTGG-3' (sense).

#### 2.3 Cell Culture and shRNA Transfection

The HeLa cell line (CL-0101; Procell, Wuhan, China) was validated by STR profiling and tested negative for mycoplasma, and then cultured at 37 °C with 5% CO<sub>2</sub> in RPMI-1640 medium (CM-0063; Procell) supplemented with 10% fetal bovine serum (10091148; Gibco, Beijing,

China), 100 µg/mL streptomycin, and 100 U/mL penicillin (SV30010; Hyclone, Logan, UT, USA). Then shRBM6 and shNC were transfected into HeLa cells using Lipofectamine 2000 (Invitrogen, Carlsbad, CA, USA) according to the manufacturer's protocol. After 48 h, the HeLa cells were collected for subsequent experiments and analysis.

#### 2.4 Cell Proliferation Assay

The cell proliferation assay was performed as previously described [25] using the Cell Counting Kit-8 assay (40203ES76; Yeasen, Shanghai, China). Briefly, shRBM6-and shNC-transfected HeLa cells were seeded in culture plates at a density of 10,000 cells/well. After 24, 48, and 72 h of incubation, 10  $\mu$ L CCK-8 solution was added to the cells followed by incubation for an additional 3 h at 37 °C. Then the optical density (OD) was measured at an absorbance of 490 nm using a microplate reader (ELX800; Biotek, Winooski, VT, USA). The OD values were used to calculate the proliferation rate.

#### 2.5 Cell Apoptosis Assay

Apoptotic cells were stained using the Annexin V-PE/7-AAD Apoptosis Detection Kit (KGA-1017; Key-GEN, Nangjing, China) after 72 h of transfection. Then the shRBM6- and shNC-transfected cells (2  $\times$  10<sup>5</sup>) were incubated with 5  $\mu$ L 7-AAD suspended in 50  $\mu$ L binding buffer per sample for 15 min, and then incubated with 1  $\mu$ L Annexin V-PE (BD Pharmingen, San Diego, CA) and 450  $\mu$ L binding buffer per sample for 15 min. Flow cytometry was used to detect cell apoptosis levels for each sample.

#### 2.6 RNA Extraction, Library Construction and Sequencing

DNA was removed by RQ1 DNase (Promega Corp., Madison, WI, USA) to extract total RNA. After quality and quantity assessment of RNA by the SmartSpec Plus spectrophotometer (BioRad Laboratories, Inc., Hercules, CA, USA), we used 1 µg integral RNA for RNA-seq library construction with the NEBNext® Ultra™ Directional RNA Library Prep Kit for Illumina® (#E7420; New England Biolabs, Ipswich, MA, USA) by purifying polyadenylated RNAs. Then the RNAs were fragmented and converted into cDNAs. After end repair and A tailing, the DNAs were ligated with the Diluted NEBNext® Adaptor (New England Biolabs, Ipswich, MA, USA). The ligation products corresponding to 300-500 base pairs and digested with heatlabile uracil-DNA glycosylase, were processed and stored at -80 °C for sequencing. For next-generation sequencing, the libraries were applied to the Illumina NovaSeq 6000 sequencing system (Novogene, Beijing, China) for 150 nucleotide (nt) paired-end sequencing.

#### 2.7 RNA-seq Raw Data Cleaning and Alignment

We initially discarded raw reads with N bases, removed adaptors and low-quality bases using FASTX-Toolkit (version 0.0.13, https://github.com/Debian/fastx-t



oolkit), and finally kept reads longer than 16 nt. The quality filtered reads were aligned to the GRCh38 genome by HISAT2 [26]. Mapped reads with only one genomic location were used to calculate the read count of genes and the normalized fragments per kilobase of transcript per million fragments mapped (FPKM).

#### 2.8 AS Analysis

We used the splicing site usage variation analysis (SUVA, version 1.0.0, https://github.com/ablifedev/SUV A) pipeline [27] to calculate and quantify the AS events (ASEs) and RASEs (*p*-value < 0.05) between shRBM6 and shNC samples, including the alternative 5' splice site (alt5p), alternative 3' splice site (alt3p), overlapped (olp), intron retention (ir), and contained splice junction (contain), which are fully explained in the SUVA paper. The frequency and proportion of each SUVA ASE read (pSAR) were used to analyze statistical significance. Meanwhile, we also calculated the canonical AS types, including intron retention (IntronR), alternative 5' splice site (A5SS), alternative 3' splice site (A3SS), exon skipping (ES), mutual exclusive exon (MXE), cassette exon, A5SS&ES, A3SS&ES, 5' MXE (5pMXE), and 3' MXE (3pMXE).

#### 2.9 Differentially Expressed Gene Analysis

The differentially expressed genes (DEGs) were predicted using the DEseq2 software package (version 1.42.0, https://github.com/thelovelab/DESeq2) [28], which analyzes the differential expression of genes. A two-fold change (FC) and false discovery rate (FDR) <0.05 were selected as the cutoffs.

#### 2.10 The iRIP-seq Technique

The iRIP-seq technique was conducted as previously described [29]. Briefly, after irradiation at 400 mJ/cm<sup>2</sup>, the HeLa cells were lysed in cold wash buffer supplemented with RNase inhibitor (2313U; Takara Bio Inc., Shiga, Japan) and protease inhibitor cocktail (B14001; Bimake, Shanghai, China) on ice for 30 min. Then the RNA/protein mixture was vibrated vigorously and centrifuged to remove cell debris. Then RNAs were digested by MNase and RNaseT1 (Thermo Fisher Scientific, Waltham, MA, USA). Ethylenediamine tetra-acetic acid (EDTA, Sangon Biotech., Shanghai, China) was added to stop the digestion. The supernatant was incubated with 13 µg RBM6 antibody (14360-1-AP; Proteintech, Hongkong, China) and control IgG-antibody (AC005; ABclonal, Wuhan, China) overnight at 4 °C. After applying the mixture to the magnet and removing the supernatants, the beads were sequentially washed twice with lysis buffer. Next, the suspension was incubated in a heat block to release the immunoprecipitated RBPs with crosslinked RNAs and vortexed for 30 min. Proteinase K (Sangon Biotech., Shanghai, China) was added to the 10% input (without being immunoprecipitated) and immunoprecipitated RBM6 with crosslinked RNAs. The

RNAs were purified with phenol: chloroform: isopentyl alcohol (25:24:1 pH <5; Solarbio, Beijing, China).

The cDNA libraries were prepared with the KAPA RNA Hyper Prep Kit (KK8541, Roche, Basel, Switzerland) according to the manufacturer's instructions. Then the libraries were prepared following the manufacturer's instructions and applied to the Illumina NovaSeq sequencing system for 150 nt paired-end sequencing.

#### 2.11 iRIP-seq Data Analysis

We aligned the quality filtered reads onto the genome by HISAT2 (version 2.2.1, https://github.com/DaehwanKi mLab/hisat2) [26], kept the uniquely aligned reads, and removed the PCR duplicates with the same aligning position. Then, Piranha was used to perform peak calling between RBM6-IP and input samples [30]. The target genes of RBM6 were finally determined by the peaks. The binding motifs of RBM6-bound peaks were called by HOMER software (version 4.10, https://github.com/javrodriguez/HOMER) [31].

#### 2.12 Reverse Transcription and Quantitative PCR

Quantitative PCR (qPCR) was conducted as previously described [32]. Briefly, cDNAs were synthesized on a thermocycler (T100; Bio-Rad, Hercules, CA, USA) using a Reverse Transcription kit (R323-01; Vazyme Biotech, Nanjing, China), and qPCR was performed on the ABI QuantStudio 5 Real-Time PCR System (Thermo Fisher Scientific) following the standard operational process. The concentration of each transcript or splicing event was normalized to glyceraldehyde-3-phosphate dehydrogenase (GAPDH), and their levels were calculated using the  $2^{-\Delta\Delta CT}$  method [33]. The unpaired and two-tailed Student's *t*-test were used to compare the significant differences of each transcript or splicing event, the primer sequences are presented in **Supplementary Table 1**. Each sample had three technical replicates.

#### 2.13 Functional Enrichment Analyses

Gene Ontology (GO) and Kyoto Encyclopedia of Genes and Genome (KEGG) databases were used to calculate functions and enriched score and significance for each functional pathway using the KOBAS 2.0 server [34]. The statistical significance of each pathway was defined using hypergeometric tests and the Benjamini-Hochberg FDR controlling procedure (corrected p < 0.05).

#### 2.14 Statistical Analyses

The two-tailed unpaired Student's t-test was used for other comparisons that were not defined above between the shRBM6 and control groups. The threshold for a statistically significant difference was set as p < 0.01 or FDR < 0.05.



#### 3. Results

3.1 Higher Expression of RBM6 is Associated with a Better Prognosis in Multiple Cancer Types by Pan-Cancer Analysis

Previous studies have demonstrated that RBM6 can serve as a tumor suppressor and repress tumor growth and progression [22,23,35]. We compared RBM6 expression in tumor vs. adjacent normal samples in 24 cancer types from TCGA. Among the 24 cancer types, *RBM6* expression was upregulated (p < 0.05) in 7 cancer types and downregulated in 5 cancer types (Fig. 1A). Prognosis analysis revealed that higher RBM6 expression was significantly and positively associated with longer overall survival in 12 of the 18 cancer types (p < 0.05), including head and neck squamous cell carcinoma (HNSCC; Fig. 1B), lung adenocarcinoma (LUAD; Fig. 1C), pancreatic adenocarcinoma (PAAD; Fig. 1D), and other cancer types (Supplementary Fig. 1). Meanwhile, higher expression of *RBM6* was associated with a worse prognosis in the other six cancer types (Supplementary Fig. 1). These results demonstrate that *RBM6* expression is related to the prognosis of multiple tumors and may play an important regulatory role in the pathogenesis or development of many tumors.

## 3.2 Knockdown of RBM6 Significantly Promotes Proliferation and Inhibites Apoptosis

To further investigate the functions of RBM6 in tumor cells, we constructed an RBM6 knockdown (shRBM6) cell model by transfecting an RBM6-shRNA sequence into HeLa cells; HeLa cells transfected with an empty vector were served as the NC. We assessed the knockdown efficiency of shRBM6 by the real-time polymerase chain reaction (RT-PCR) and found that RBM6 was significantly down regulated in the shRBM6 samples (p < 0.0001; Fig. 2A). We performed flow cytometry analysis and the CCK8 assay to determine whether RBM6 could modulate cell apoptosis (Fig. 2B) and proliferation of HeLa cells, respectively. The results demonstrated that the apoptotic cell percentage was significantly decreased in shRBM6 samples (p < 0.01; Fig. 2B and Supplementary Fig. 2), whereas the cell proliferation rate reflected by the optical density was significantly increased in the shRBM6 samples (p < 0.01; Fig. 2C). These results indicate that RBM6 has a suppressive role in the tumor phenotype or function of HeLa cells.

## 3.3 RBM6 Regulates the AS of Genes Enriched in DNA Damage Response and Cellular Survival-Related Pathways

To further elucidate how RBM6 modulates the synthesis and processing of RNA in HeLa cells, we performed unbiased RNA-seq analysis for shRBM6 and normal controls (NC) HeLa cells by capturing the total polyadenylated RNAs, with three biological replicates for each group. After quality filter and genome alignment of the raw RNA-seq data, more than 95% of the aligned reads had a uniquely

aligned location in the genome and were used for further analyses (**Supplementary Table 2**). By calculating the read count and FPKM value for each gene, we detected a total of 28,218 expressed genes from the six RNA-seq samples (**Supplementary Table 3**). We presented the FPKM values of *RBM6* and confirmed its successful knockdown from the RNA-seq analysis results (Fig. 3A).

As an AS factor, RBM6 is supposed to modulate the tumorigenesis or development probably by playing an essential role in regulating the AS profile. Since cancers undergo complex splicing events [36], we detected thousands of ASEs in RNA-seq using SUVA [27] (Supplementary Fig. 3A). Among these ASEs, 1897 high-confidence RASEs were identified by applying stringent cutoffs of  $p \le$ 0.05 and splicing ratio difference  $\geq$ 0.15 (Supplementary **Table 4**, Fig. 3B). There were 5 RASE types: 852 alt3p, 818 alt5p, 95 contain, 19 IR, and 113 olp. Strikingly, 11.4% of SUVA RASEs were simple and 88.6% were complex. Complex events contained splicing junctions that were involved in two or more splicing events (Fig. 3C), indicating that RBM6 prefers to regulate the complex ASEs in HeLa cells. We then corresponded the SUVA RASEs to classical splicing events, with A5SS, A3SS, ES, and cassette exon events accounting for a large proportion (Fig. 3D and Supplementary Fig. 3B). One splicing event was involved in two or more transcripts, whereas only one transcript was probably highly expressed and dominantly spliced for this gene. Thus, we decided to predict the dominant transcript undergoing AS that could be quantified by the "pSAR" value using SUVA. We calculated the number of RASEs with different pSAR values, and found that 598 dominant splicing events had pSAR  $\geq$ 50% (Fig. 3E). These 598 RASEs were selected for further analyses. Meanwhile, we performed principal component analysis (PCA) for RASEs and found that the shRBM6 group and the control group were clearly separated by the splicing ratio of these 598 RASEs (Fig. 3F and Supplementary Fig. 3C).

These 598 RBM6-RASEs were distributed in 463 genes, which were enriched in GTPase and transcription pathways (Fig. 3G). We found that RBM6 regulates the AS of many genes involved in proliferative and apoptotic processes (Fig. 3H). The reads distribution diagram showed an RASE in the membrane associated ring-CH-type finger 7 (MARCHF7) gene, and the splicing model showed the significantly dysregulated splicing pattern of this event (Fig. 3I). In such a complex AS region, SUVA identified the RASE that was significantly altered between the shRBM6 and control samples. As shown in Fig. 3I, the exons shown as black boxes were skipped after knocking down RBM6. Another RASE, located in *PRKCD*, showed a tendency for intermediate exons (Supplementary Fig. 3D). These results indicate that RBM6 may affect the survival and development of cancer cells by regulating variable splicing of genes involved in cell proliferation or apoptosis.



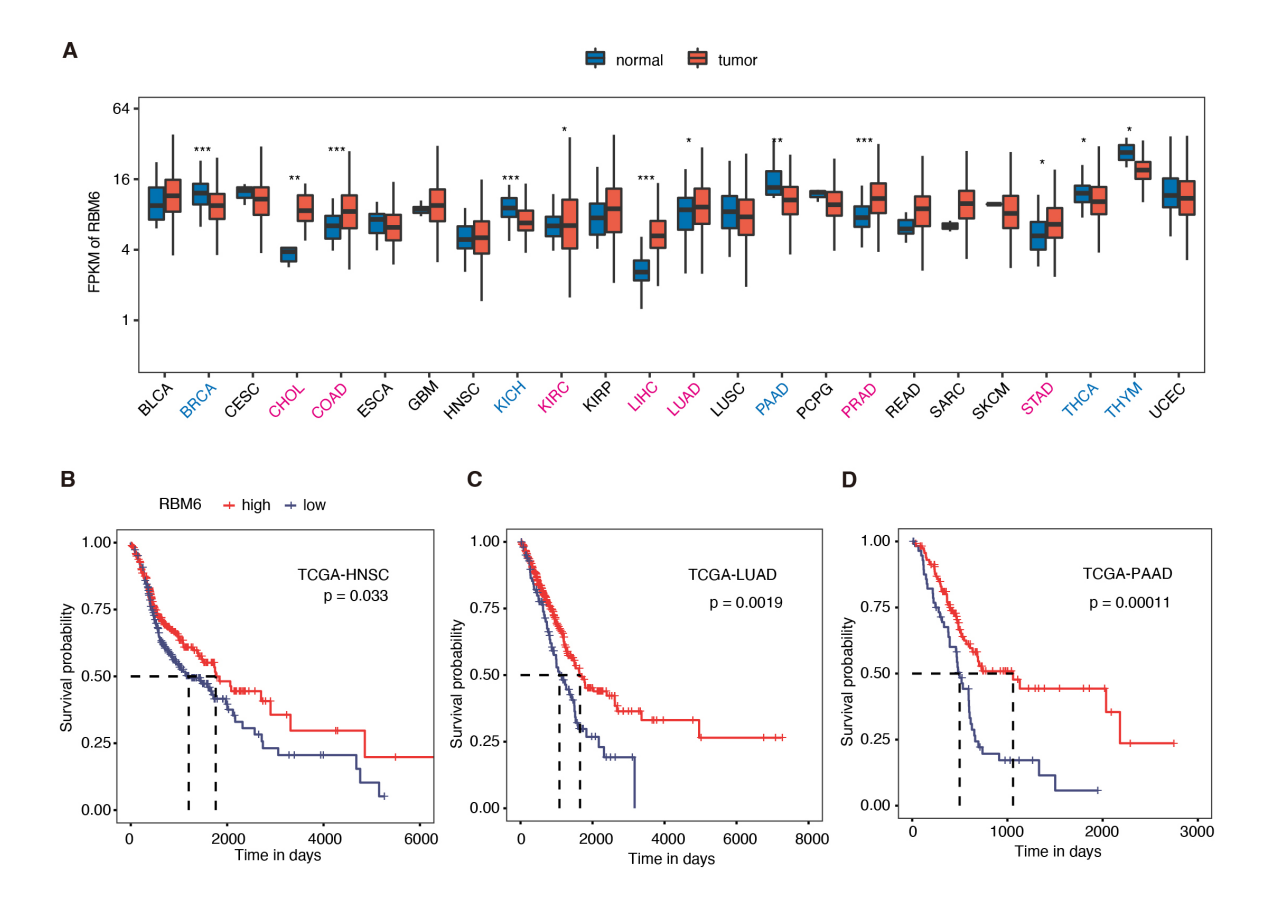


Fig. 1. Higher RBM6 expression was associated with better prognosis in several tumor types by pan-cancer analysis. (A) The boxplot shows RBM6 expression pattern in tumor vs. normal tissues in the 24 cancer types from TCGA. RBM6 expression was upregulated in seven cancer types, and down-regulated in five cancer types. \* p < 0.05; \*\*\* p < 0.01; \*\*\*\* p < 0.001; Student's t-test. (B) The survival curve displays the prognosis of HNSCC from TCGA. (C) The same as (B) but for LUAD. (D) The same as (B) but for pancreatic adenocarcinoma. RBM6, RNA-binding motif protein 6; TCGA, The Cancer Genome Atlas; HNSCC, head and neck squamous cell carcinoma; LUAD, lung adenocarcinoma.

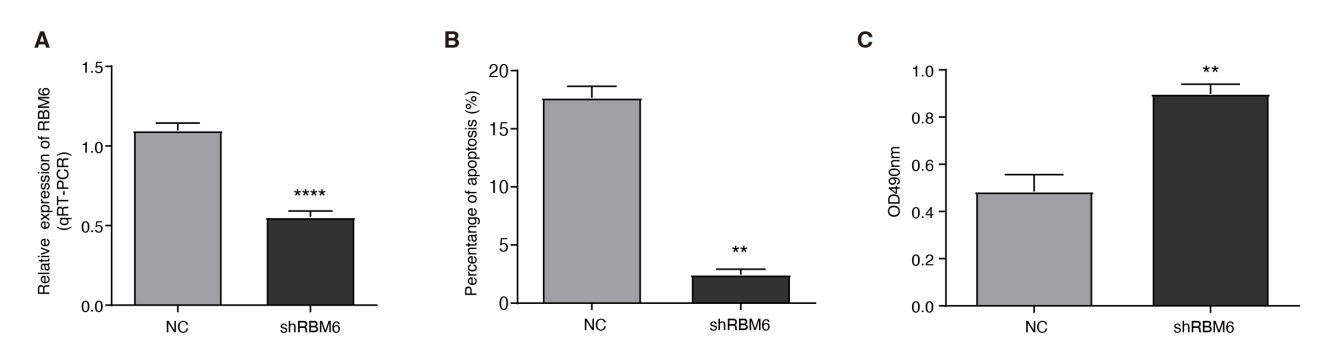


Fig. 2. RBM6 knockdown promoted proliferation and inhibited apoptosis. (A) The bar plot shows reverse transcription and quantitative polymerase chain reaction (RT-qPCR) validation of RBM6 knockdown efficiency. (B) The bar plot shows the decreased cellular apoptosis rate in the shRBM6 group. (C) The bar plot indicates the increased cellular proliferation level in the shRBM6 group. The values are presented as the mean  $\pm$  standard deviation. \*\* p < 0.01; \*\*\*\* p < 0.0001; Student's t-test.

3.4 RBM6 Regulates the Expression of Genes Associated with Tumor Development, which may be Mediated by TFs from RBM6-RASEs

To investigate RBM6-mediated transcriptional regulation, the DESeq2 package was used to identify the DEGs between shRBM6 and NC samples using FC  $\geq$ 2 and FDR

<0.05 as criteria [28] (**Supplementary Fig. 4A**). We finally obtained 202 up-regulated and 1348 down-regulated DEGs (Fig. 4A, **Supplementary Table 5**), indicating that RBM6 knockdown tended to result in repression of gene expression as there were more downregulated than upregulated DEGs.



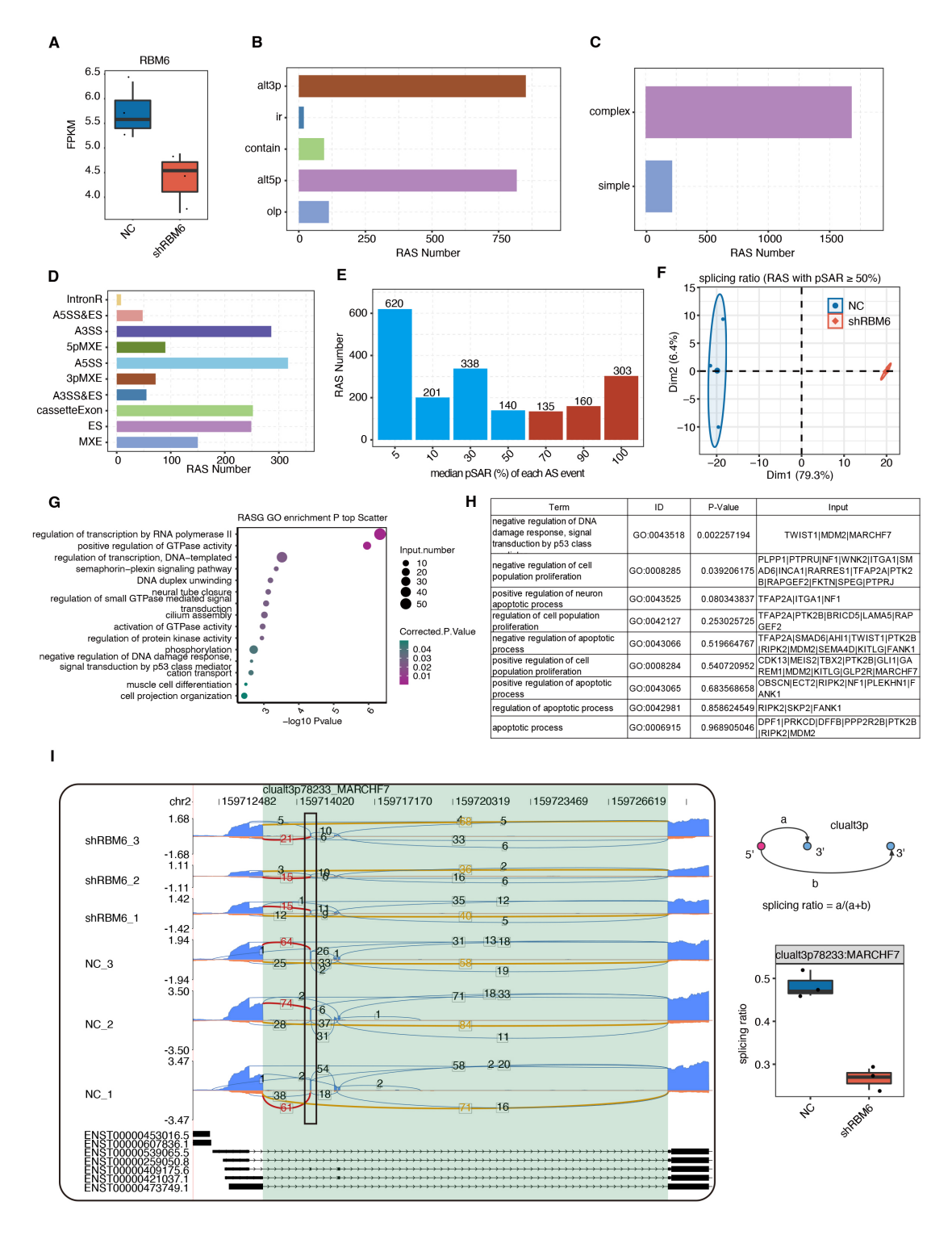


Fig. 3. RBM6 modulated the AS pattern of genes enriched in DNA damage response- and cell survival-related pathways. (A) Boxplot shows the Fragments per kilobase per million mapped (FPKM) of RBM6. (B) Barplot shows the number of RASEs detected by SUVA between shRBM6 and NC. (C) Barplot presents the number of RASEs by dividing them into complex and simple ASEs using SUVA. (D) Barplot shows the corresponding classical ASE types for the RASEs detected by SUVA. (E) Barplot shows the number of RASEs with increased pSAR values. RASEs with pSAR  $\geq$ 50% are labeled as brown. (F) PCA clustering of RASEs with pSAR  $\geq$ 50%. (G) The bubble plot displays the top 10 GO pathways for RASGs (pSAR  $\geq$ 50%) in the shRBM6 vs. NC groups. (H) The table shows proliferation and apoptosis pathways in the shRBM6 group. (I) Read distribution diagram shows clualt3p78233 MARCHF7. The boxplot in the right panle shows the splicing ratio of clualt3p78233 MARCHF7. AS, alternative splicing; RAS, regulated AS; RASEs, RBM6-regulated AS events; SUVA, site usage variation analysis; NC, negative control; ASEs, AS events; pSAR, proportion of each SUVA ASE read; PCA, principal component analysis; GO, Gene Ontology; RASGs, The genes involve RASE.

To further identify the potential functions of these DEGs, we performed GO (Supplementary Table 6) and KEGG (Supplementary Table 7) enrichment analyses. The top 10 upregulated- and downregulated GO terms and the top 10 upregulated- and downregulated KEGG pathways were shown in Fig. 4B,C and Supplementary Fig. 4B,C, respectively. The up-regulated genes in the shRBM6 cells are primarily enriched in type I interferon (IFN) signaling pathways, defense response to virus, and the innate immune response (Fig. 4B). Type I IFN is tightly associated with viral infection and has double-edged effects on tumor development and resistance to treatment [37,38]. Interestingly, the down-regulated DEGs were mainly associated with cell cycle and DNA damage response (DDR) pathways, including cellular responses to DNA damage stimulus, cell cycle, and DNA repair. Positive regulation of GTPase activity, RNA splicing, and cilium assembly were also enriched in the down-regulated DEGs (Fig. 4C). Cellular responses to DNA damage stimulus are closely related to apoptosis in multiple cancers [39,40]. These results suggest that shRBM6 can activate the type I IFN signaling pathway and suppress the DDR, ultimately inhibiting the apoptosis of cancer cells. Meanwhile, we also found that the expression of many oncogenes or tumor suppressor genes was detected in the DEGs caused by shRBM6 (Fig. 4D and Supplementary Fig. 4D).

RBM6 is an important AS regulator. The genes involve RBM6-RASE (RASGs) were enriched in transcriptional regulatory pathways (Fig. 3G). We speculate that the AS of many transcription factors (TFs) is regulated by RBM6, which in turn has an impact on the transcriptome. In total, 63 of 464 RASGs were identified as TFs (Fig. 4E). We conducted a correlation analysis of the expressions of DEGs and the splicing ratios of RASEs from these 63 TFs (Pearson's correlation coefficient >0.8, p < 0.01). Meanwhile, TF-target pairs of these 63 TFs with RASEs were selected from three databases (TRRUST, Encode, and TF-BSDB). Finally, 202 TF-target pairs were identified and the co-disturbed network was constructed (Fig. 4F). To confirm the dysregulation by shRBM6, we performed RT-qPCR and validated the decreased expression of interleukin 24 and ETS1, and increased expression of interferon regulatory factor 7 (IRF7) (Fig. 4G). Based on these results, we propose that RBM6 may indirectly play a regulatory role at the transcriptional level through regulating the splicing of these TFs (Supplementary Fig. 4E).

### 3.5 RBM6-RNA Global Interaction Exploration in HeLa Cells

To study the RBM6-RNA interactions and the mechanism underlying the function of RBM6, we obtained the global RBM6-RNA interaction profile in HeLa cells by iRIP-seq [29,41]. We used ultraviolet cross-linking and RNA digestion to capture the exact RNA-protein interaction locations. The iRIP cDNA libraries were sequenced on

the Illumina platform, generating abundant iRIP-seq reads for RBM6 IP and input control samples with two biological replicates for each (Supplementary Table 8). We processed and aligned the cDNA sequence reads to the human GRCh38 genome using HISAT2. The fractions of the aligned reads were 78.14-86.99%, from which we selected the uniquely aligned reads for following analyses (Supplementary Table 8). By classifying the uniquely mapped reads to the genomic location, we found that the RBM6-associated reads showed a higher percentage in the 5'UTR and intergenic regions but lower percentage in the intron and coding sequence (CDS) regions (Fig. 5A). The normalized reads density along the uniformed gene region showed that RBM6 had a stronger tendency for the 5'UTR regions compared with the CDS and 3'UTR regions (Fig. 5B).

To further elucidate the characteristics of the RBM6-RNA interaction, we called the RBM6-binding peaks from iRIP-seq reads using Piranha. In total, 584 shared peaks between the two replicates were identified (Fig. 5C). The genomic locations of these peaks showed that most of these peaks came from the antisense, CDS and intron regions (Fig. 5D). Further analysis showed that RBM6 binding reads were slightly and specifically enriched in the transcription start site, whereas peak reads were significantly enriched in the intron region (Supplementary Fig. 5A,B). Next, we applied the HOMER algorithm to identify the enriched motif sequences over-represented in the RBM6 peaks. Consistent with a previous report [21], the CUCU motif was enriched. However, the top motif was GGC-GAUG, indicating that the motif selection could be cellular heterogeneity (Fig. 5E).

Functional clustering by GO was performed to annotate the functions of the RBM6-bound genes containing at least one RBM6 peak; the enrichment fell into the cell cycle, cell differentiation, and cell migration (Supplementary Fig. 5C). As shown in Fig. 5F, 39 RASGs overlapped with RBM6-bound genes, indicating that RBM6 might directly bind to the RNAs of these targets and regulate their AS pattern. In addition, several genes were found to be involved in proliferation or apoptosis, including cyclindependent kinase 13 (CDK13), laminin subunit alpha 5 (LAMA5), obscurin (OBSCN), SMAD Family Member 6 (SMAD6), and transcription factor AP2 (TFAP2A). Four TFs, AT-Hook DNA Binding Motif Containing 1 (AHDC1), SMAD6, TFAP2A, and zinc finger protein 276 (ZNF276), were also directly bound by RBM6. Visualization of the reads profile showed an RASE in ZNF276 and RBM6binding profiles (Fig. 5G). RBM6 specifically binds to the first 5' exon at the proximal end, and this exon is more selected in the control group, whereas the first 5' exon at the distal end is more selected after RBM6 knockdown.



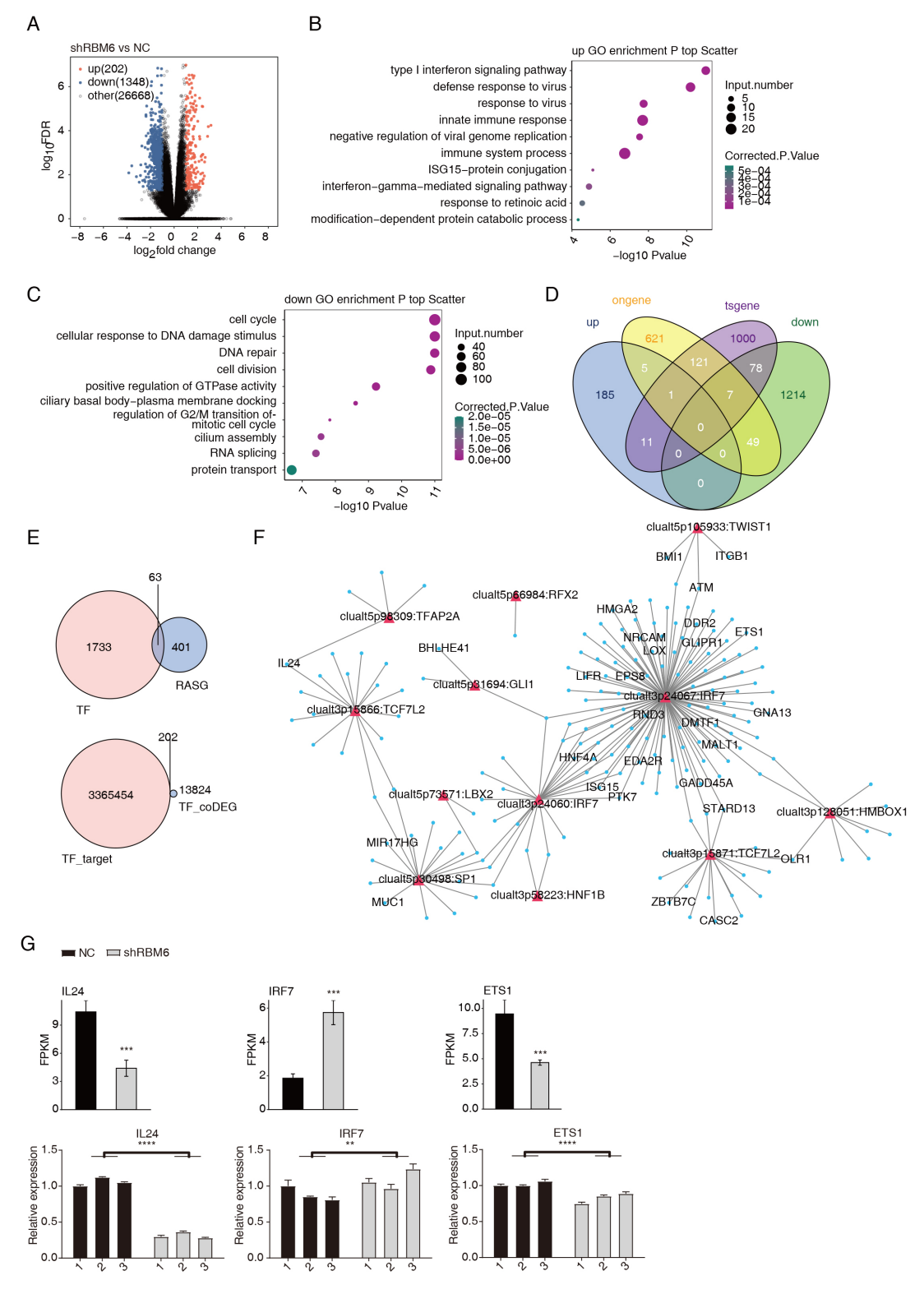


Fig. 4. RBM6 significantly altered the expression of genes associated with tumor development, which may be mediated by TFs from RBM6-RASGs. (A) Volcano plot presents the upregulated- and downregulated-DEGs in the shRBM6 vs. NC groups using DE-Seq2. (B) The top 10 enriched GO pathways of up-regulated DEGs in the shRBM6 group. (C) The top 10 enriched GO pathways of down-regulated DEGs in the shRBM6 group. (D) Venn diagram shows the upregulated- and downregulated-genes and the known oncogenes or tumor suppressor genes. (E) Venn diagram shows the overlap of TFs and RASGs. Venn diagram showing the overlap of TF-targets and DEGs (above). Venn diagram shows TF-targets and TF-related DEGs overlay (below). (F) Network showing TF-target pairs were screen out and the co-disturbed. (G) Bar plot showing the RT-qPCR results. TF, ranscription factors; DEGs, differentially expressed genes (\*\* p < 0.01; \*\*\*\* p < 0.001; \*\*\*\* p < 0.0001.)

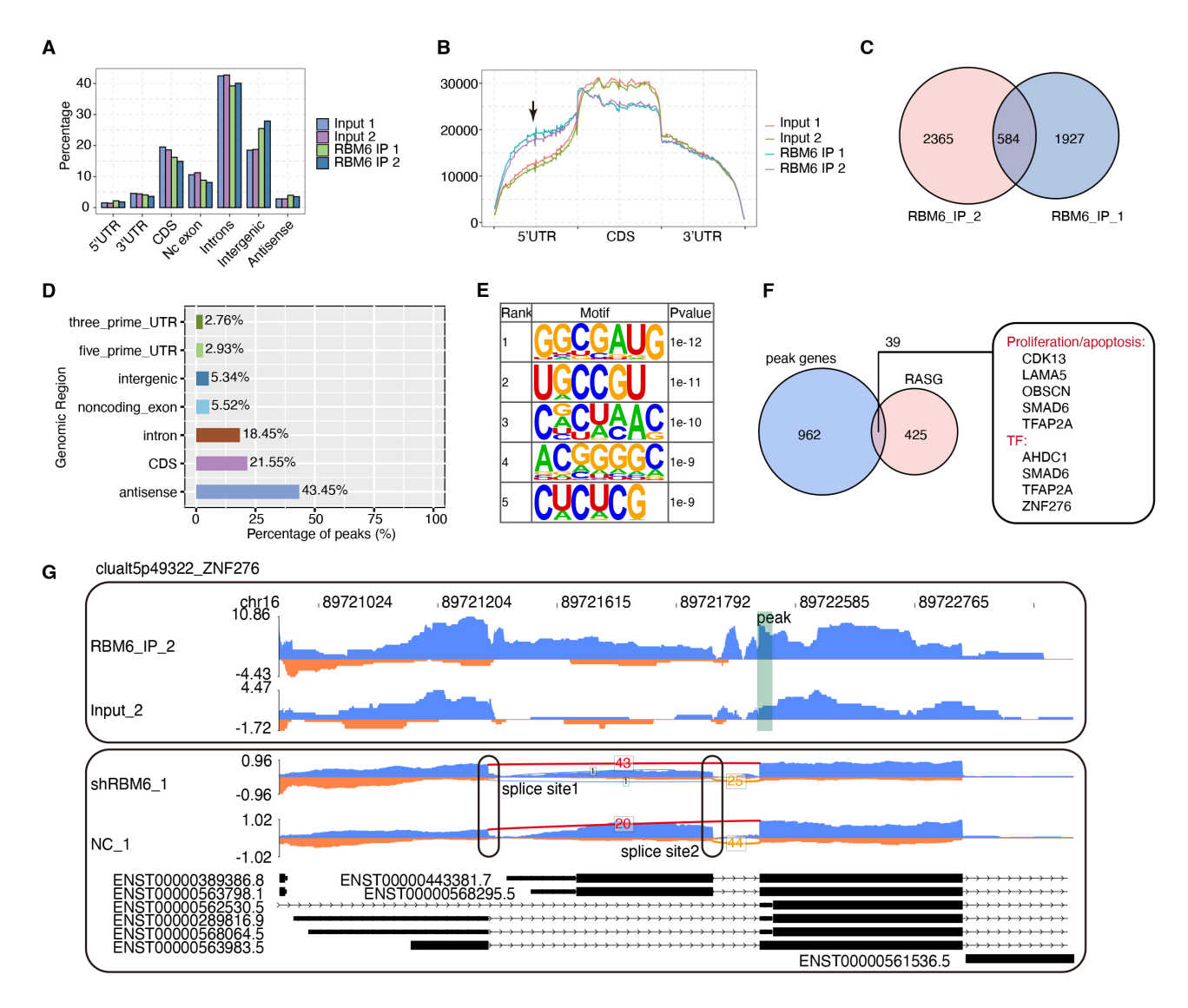


Fig. 5. RBM6-mRNA interaction map in HeLa cells. (A) Barplot shows the distribution of sequencing reads on different genome regions. (B) Coverage intensity analysis of iRIP-seq reads with the length of the transcription unit was carried out. The 5'UTR, CDS, and 3'UTR of the gene were divided into 100 evenly, each of which was called a bin. The sum of the average reads in each bin was calculated to obtain the overall reads coverage. (C) Venn diagram shows the common and unique peaks in two IP replicate treatment groups by using the Piranha method. The peaks with overlapping positions are clustered in the two replicates, and the overlapping peaks are classified under the same cluster. (D) The proportion of peak reads in different regions of the genome. (E) The top five enriched motifs in the overlapped RBM6 peaks. (F) RASGs co-expressing with RBM6 were screened. Venn diagram shows the peaks bound by RBM6-RASGs. (G) Reads plot shows one RASE in the ZNF276 and RBM6 binding profiles. iRIP-seq, RNA immunoprecipitation coupled with sequencing; CDS, coding sequence; IP, immunoprecipitation; ZNF276, zinc finger protein 276.

#### 4. Discussion

In this study, we investigated whether RBM6 can exercise functions through transcriptional or post-transcriptional regulation in HeLa cells. According to pancancer data from TCGA, *RBM6* was upregulated in 7 of 24 cancer types and downregulated in 5 cancer types and higher *RBM6* expression was positively correlated with a better prognosis. These results indicate that RBM6 may have an important role in tumor development. Based on this hypothesis, the HeLa cell model was used to analyze

the cellular phenotypes and molecular alterations by knocking down *RBM6* with shRNA. ShRBM6 promoted cell proliferation and inhibited cell apoptosis. Furthermore, using RNA-seq, we found that shRBM6 regulated AS pattern of genes involved in cell proliferation and apoptosis pathways, as well as genes involved in transcriptional regulation. The up-regulated DEGs were enriched in the Type I IFN pathway and the down-regulated DEGs were enriched in the DDR pathway. These results suggest that as a splicing factor, RBM6 may regulate the splicing of TF-associated



genes. To further investigate how RBM6 plays a role using its RNA binding activity, we analyzed the binding peaks of RBM6 by iRIP-seq reads using the Piranha pipeline [30]. The results showed that RBM6 could bind to genes related to cell apoptosis, cell proliferation, and TFs.

RBM6 is a tumor suppressor gene in multiple cancers. For example, RBM6 can repress the progression of laryngeal carcinoma [22] and HCC [23]. Moreover, overexpression of RBM6 can inhibit cell proliferation and promote the apoptosis of HepG2 cells and HCC tissues [42]. Through pan-cancer analysis, we found that RBM6 expression differs in cancer and adjacent tissues. Meanwhile, higher expression of RBM6 was associated with a better prognosis in most cancers, consistent with previous reports. However, it should be noticed that RBM6 can also promote the progression of tumors in specific cancer types. In this study, we found that higher expression of RBM6 was correlated with a better prognosis, suggesting that RBM6 primarily plays a tumor-suppressor role in multiple cancer types. Meanwhile, we found that knocking down RBM6 promoted cell proliferation and inhibited cell apoptosis, which illustrated the tumor-suppressor function of RBM6 in HeLa cells. The result was consistent with the prognostic analysis. At the same time, additional experiments such as cellular invasion, migration, and scratch assays are also necessary to perform in future studies to confirm the tumor-suppressor function of RBM6.

As a splicing factor, RBM6 participates in the regulation of AS [16-19]. RBM6 regulates the AS-coupled nonstop decay of a positive homologous recombinational repair (HRR) regulator, Fe65/amyloid beta A4 precursor proteinbinding family B member 1, and RBM6 knockdown significantly reduces Fe65 protein levels, consequently impairing the HRR of DNA double strand breaks [24]. It is also known that RBM6 modulates the proliferation, migration, and apoptosis of tumor cells by regulating RNA metabolism [43]. This is the first study to analyze the transcriptome regulated by RBM6 at the genome-wide level in HeLa cells through high-throughput sequencing. We found that RBM6 regulates the AS of many proliferation- and apoptosisrelated genes, such as MARCH7, which promotes cell proliferation and invasion through VAV2-RAC1-CDC42 pathway in cervical cancer cells [44]. Moreover, TFAP2A regulates the growth and survival of nasopharyngeal carcinoma by regulating the hypoxia inducible factor- $1\alpha$  (HIF- $1\alpha$ )mediated vascular endothelial growth factor/pigment epithelium derived factor (VEGF/PEDF) signaling pathway, indicating that TFAP2A is a potential therapeutic maker and prognostic target in tumor [45]. TFAP2A isoforms may be differentially regulated during tumor development. The differentially regulated TFAP2A isoforms and their different transcriptional activity may affect tumor responses to drug therapy [46,47]. We did not confirm these dysregulated ASEs by assessing changes at the mRNA or protein level, which could be performed in future studies.

Interestingly, knocking down the expression of *RBM6* also up-regulates the expression of genes involved in the type I IFN pathway. Type I IFNs have been extensively studied for their association with tumor progression [48]. They reportedly contribute to immune cell exhaustion and other harmful effects by prolonged stimulation, thus directly or indirectly allowing cancer cells to escape immune clearance [49]. In the present study, up-regulated genes caused by shRBM6 were mostly enriched in the type I IFN signaling pathway, which suggests that RBM6 knockdown may enhance the ability of cancer cells to escape immune clearance. Furthermore, we found that genes associated with up-regulated type I IFNs include OAS1, OAS2, IFITM1, IFI6, and IRF7. These 5 up-regulated genes are associated with tumor initiation and progression [50–55], indicating the beneficial effect of RBM6 on the apoptosis of cancer cells.

DDR is an essential function in the maintenance of genome stability in cancer cells [56]. Since aberrant pericellular development is a basic mechanism of tumorigenesis, the cell cycle regulation has become a key target for anti-cancer therapy [57]. In this study, we found that after RBM6 knockdown, genes involved in DDR and cell cycle pathways were significantly down-regulated. Inhibition of DDR genes by shRBM6 may inhibit the activation of p53, thus inhibiting the apoptosis of cancer cells [58]. DDR- and cell cycle-related genes include GADD45A, INO80, EID3, and BCCIP. GADD45A is a p53 effector gene that has protective effects on cancer [59] by mediating cell cycle arrest and inducing apoptosis. INO80 is required for cell cycle control [60]. EID3 has effects on cell proliferation, cell cycle, cell apoptosis, and promotes treatment resistance to the maintenance of cancer stem cell characteristics [61]. The high expression of BCCIP indicates a poor prognosis and promotes the proliferation and migration of LUAD cells [62]. It has been reported that the TFs involved in myogenic transcription are regulated by the AS of their transcripts. The AS of many transcripts is aberrant in neuromuscular pathology [63]. As a splicing factor, RBM6 may regulate transcription by regulating the AS of TFs. In this study, we constructed a co-disturbed network between the DEGs and AS of TFs regulated by RBM6.

RBM6 reportedly controls the proliferation of HeLa cancer cells, and the crosslinking-immunoprecipitation and high-throughput sequencing (CLIP-seq) has shown that RBM6 has a binding preference for the CUCUGAA sequence [21]. In this study, we used the iRIP-seq dataset to identify both directly and indirectly interacting RNA targets with RBM6. The results demonstrated that RBM6 interacted with many mRNAs and pre-mRNAs, with an mRNA binding preference and genomic location towards the 5'UTR. Motifs analysis revealed that RBM6-bound RNAs are enriched in GGCGAUG and CUCU motifs, which may be caused by the different binding effects of RBM6 on different cells. RBM6-bound mRNAs/pre-



mRNAs, which involve regulated AS, are enriched in proliferation and apoptosis pathways (*CDK13*, *LAMA5*, *OBSCN*, *SMAD6*, *TFAP2A*) and the TFs (AHDC1, ZNF276, SMAD6 and TFAP2A). CDK13 promotes DNA damage and cell death in triple-negative breast cancer, thus serving as a therapeutic target [64]. *LAMA5* could be a potential prognostic factor in ovarian cancer [65]. Patients with gastric adenocarcinoma with OBSCN mutations have good treatment effects and prognoses [66]. These TFs binding to RBM6 could promote the growth of tumor cells [67–70]. Together, these results support the hypothesis that RBM6 may play a role in tumor growth by encoding its RNA binding activity either directly or indirectly.

#### 5. Conclusions

In summary, our study analyzed the RNA binding properties and molecular functions of RBM6 in HeLa cells. RBM6 regulation of the transcriptome was tightly associated with its cellular functions in HeLa cells. In future research, we plan to further investigate how RBM6 binds to the TFs and genes associated with proliferation and apoptosis and the mechanisms underlying the role of RBM6 in cancer.

#### Availability of Data and Materials

The datasets presented in this study can be found in online repositories. The names of the repository/repositories and accession number(s) are: Gene Expression Omnibus (GEO), accession number: GSE223199. The datasets used and/or analyzed during the current study are available from the corresponding author on reasonable request.

#### **Author Contributions**

DL conceived and designed the experiments and revised the manuscript; PP, WS, and JH performed the experiments; QY, CC, and HG analyzed the data; PP wrote the paper. All authors have read and approved the final manuscript. All authors contributed to editorial changes in the manuscript. All authors have participated sufficiently in the work and agreed to be accountable for all aspects of the work.

#### **Ethics Approval and Consent to Participate**

Not applicable.

### Acknowledgment

We are very grateful to technicians from Wuhan Ruixing Biotechnology Co. for their help in generating data presented in this study.

#### **Funding**

This work was supported by grants from the Youth Project of the National Natural Science Foundation of China (grant number 81904019).

#### **Conflict of Interest**

The authors declare no conflict of interest. Qingqing Yin and Hao Guo are employed by Wuhan Ruix- ing Biotechnology Co., Ltd, and Chao Cheng is employed by ABLife BioBigData Institute, the judgments in data interpretation and writing were not influenced by this relationship.

#### **Supplementary Material**

Supplementary material associated with this article can be found, in the online version, at https://doi.org/10.31083/j.fbl2909330.

#### References

- [1] Goodall GJ, Wickramasinghe VO. RNA in cancer. Nature Reviews. Cancer. 2021; 21: 22–36.
- [2] Qin H, Ni H, Liu Y, Yuan Y, Xi T, Li X, et al. RNA-binding proteins in tumor progression. Journal of Hematology & Oncology. 2020: 13: 90.
- [3] Hong S. RNA Binding Protein as an Emerging Therapeutic Target for Cancer Prevention and Treatment. Journal of Cancer Prevention. 2017; 22: 203–210.
- [4] Li W, Deng X, Chen J. RNA-binding proteins in regulating mRNA stability and translation: roles and mechanisms in cancer. Seminars in Cancer Biology. 2022; 86: 664–677.
- [5] Wang S, Sun Z, Lei Z, Zhang HT. RNA-binding proteins and cancer metastasis. Seminars in Cancer Biology. 2022; 86: 748– 768
- [6] Mohibi S, Chen X, Zhang J. Cancer the RBP eutics-RNA-binding proteins as therapeutic targets for cancer. Pharmacology & Therapeutics. 2019; 203: 107390.
- [7] Fredericks AM, Cygan KJ, Brown BA, Fairbrother WG. RNA-Binding Proteins: Splicing Factors and Disease. Biomolecules. 2015; 5: 893–909.
- [8] Hashimoto S, Kishimoto T. Roles of RNA-binding proteins in immune diseases and cancer. Seminars in Cancer Biology. 2022; 86: 310–324.
- [9] Ming R, Li X, Wang E, Wei J, Liu B, Zhou P, et al. The Prognostic Signature of Head and Neck Squamous Cell Carcinoma Constructed by Immune-Related RNA-Binding Proteins. Frontiers in Oncology. 2022; 12: 795781.
- [10] Ma R, Zhao LN, Yang H, Wang YF, Hu J, Zang J, et al. RNA binding motif protein 3 (RBM3) drives radioresistance in nasopharyngeal carcinoma by reducing apoptosis via the PI3K/AKT/Bcl-2 signaling pathway. American Journal of Translational Research. 2018; 10: 4130–4140.
- [11] Wang E, Aifantis I. RNA Splicing and Cancer. Trends in Cancer. 2020; 6: 631–644.
- [12] Jbara A, Lin KT, Stossel C, Siegfried Z, Shqerat H, Amar-Schwartz A, et al. RBFOX2 modulates a metastatic signature of alternative splicing in pancreatic cancer. Nature. 2023; 617: 147–153.
- [13] Cerami E, Gao J, Dogrusoz U, Gross BE, Sumer SO, Aksoy BA, *et al.* The cBio cancer genomics portal: an open platform for exploring multidimensional cancer genomics data. Cancer Discovery. 2012; 2: 401–404.
- [14] Gao J, Aksoy BA, Dogrusoz U, Dresdner G, Gross B, Sumer SO, *et al*. Integrative analysis of complex cancer genomics and clinical profiles using the cBioPortal. Science Signaling. 2013; 6: pl1.
- [15] Cancer Genome Atlas Research Network, Weinstein JN, Collisson EA, Mills GB, Shaw KRM, Ozenberger BA, et al. The Can-



- cer Genome Atlas Pan-Cancer analysis project. Nature Genetics. 2013; 45: 1113–1120.
- [16] Callebaut I, Mornon JP. OCRE: a novel domain made of imperfect, aromatic-rich octamer repeats. Bioinformatics. 2005; 21: 699–702.
- [17] Inoue A. RBM10: Structure, functions, and associated diseases. Gene. 2021; 783: 145463.
- [18] Martin BT, Serrano P, Geralt M, Wüthrich K. Nuclear Magnetic Resonance Structure of a Novel Globular Domain in RBM10 Containing OCRE, the Octamer Repeat Sequence Motif. Structure. 2016; 24: 158–164.
- [19] Mourão A, Bonnal S, Soni K, Warner L, Bordonné R, Valcárcel J, *et al.* Structural basis for the recognition of spliceosomal SmN/B/B' proteins by the RBM5 OCRE domain in splicing regulation. eLife. 2016; 5: e14707.
- [20] Heath E, Sablitzky F, Morgan GT. Subnuclear targeting of the RNA-binding motif protein RBM6 to splicing speckles and nascent transcripts. Chromosome Research. 2010; 18: 851–872.
- [21] Bechara EG, Sebestyén E, Bernardis I, Eyras E, Valcárcel J. RBM5, 6, and 10 differentially regulate NUMB alternative splicing to control cancer cell proliferation. Molecular Cell. 2013; 52: 720–733.
- [22] Wang Q, Wang F, Zhong W, Ling H, Wang J, Cui J, *et al.* RNA-binding protein RBM6 as a tumor suppressor gene represses the growth and progression in laryngocarcinoma. Gene. 2019; 697: 26–34.
- [23] Ye Z, Zhang J, Yang Y, Wei Y, Li L, Wang X. RNA-binding protein RBM6 acts as a tumor suppressor gene to inhibit the progression of hepatocellular carcinoma. Journal of B.U.ON. 2021; 26: 402–408.
- [24] Machour FE, Abu-Zhayia ER, Awwad SW, Bidany-Mizrahi T, Meinke S, Bishara LA, et al. RBM6 splicing factor promotes homologous recombination repair of double-strand breaks and modulates sensitivity to chemotherapeutic drugs. Nucleic Acids Research. 2021; 49: 11708–11727.
- [25] Saiding A, Maimaitiyiming D, Chen M, Yan F, Chen D, Hu X, *et al.* PCMT1 knockdown attenuates malignant properties by globally regulating transcriptome profiles in triple-negative breast cancer cells. PeerJ. 2023; 11: e16006.
- [26] Kim D, Langmead B, Salzberg SL. HISAT: a fast spliced aligner with low memory requirements. Nature Methods. 2015; 12: 357–360.
- [27] Cheng C, Liu L, Bao Y, Yi J, Quan W, Xue Y, et al. SUVA: splicing site usage variation analysis from RNA-seq data reveals highly conserved complex splicing biomarkers in liver cancer. RNA Biology. 2021; 18: 157–171.
- [28] Love MI, Huber W, Anders S. Moderated estimation of fold change and dispersion for RNA-seq data with DESeq2. Genome Biology. 2014; 15: 550.
- [29] Tu Y, Wu X, Yu F, Dang J, Wei Y, Yu H, et al. Tristetraprolin-RNA interaction map reveals a novel TTP-RelB regulatory network for innate immunity gene expression. Molecular Immunology. 2020; 121: 59–71.
- [30] Uren PJ, Bahrami-Samani E, Burns SC, Qiao M, Karginov FV, Hodges E, *et al.* Site identification in high-throughput RNA-protein interaction data. Bioinformatics. 2012; 28: 3013–3020.
- [31] Heinz S, Benner C, Spann N, Bertolino E, Lin YC, Laslo P, et al. Simple combinations of lineage-determining transcription factors prime cis-regulatory elements required for macrophage and B cell identities. Molecular Cell. 2010; 38: 576–589.
- [32] Li RZ, Hou J, Wei Y, Luo X, Ye Y, Zhang Y. hnRNPDL extensively regulates transcription and alternative splicing. Gene. 2019; 687: 125–134.
- [33] Livak KJ, Schmittgen TD. Analysis of relative gene expression data using real-time quantitative PCR and the 2(-Delta Delta C(T)) Method. Methods. 2001; 25: 402–408.

- [34] Bu D, Luo H, Huo P, Wang Z, Zhang S, He Z, *et al.* KOBASi: intelligent prioritization and exploratory visualization of biological functions for gene enrichment analysis. Nucleic Acids Research. 2021; 49: W317–W325.
- [35] Wang K, Ubriaco G, Sutherland LC. RBM6-RBM5 transcription-induced chimeras are differentially expressed in tumours. BMC Genomics. 2007; 8: 348.
- [36] Sterne-Weiler T, Weatheritt RJ, Best AJ, Ha KCH, Blencowe BJ. Efficient and Accurate Quantitative Profiling of Alternative Splicing Patterns of Any Complexity on a Laptop. Molecular Cell. 2018; 72: 187–200.e6.
- [37] Holicek P, Guilbaud E, Klapp V, Truxova I, Spisek R, Galluzzi L, *et al.* Type I interferon and cancer. Immunological Reviews. 2024; 321: 115–127.
- [38] Snell LM, McGaha TL, Brooks DG. Type I Interferon in Chronic Virus Infection and Cancer. Trends in Immunology. 2017; 38: 542–557
- [39] Figueroa-González G, Pérez-Plasencia C. Strategies for the evaluation of DNA damage and repair mechanisms in cancer. Oncology Letters. 2017; 13: 3982–3988.
- [40] Zhang T, Brazhnik P, Tyson JJ. Exploring mechanisms of the DNA-damage response: p53 pulses and their possible relevance to apoptosis. Cell Cycle. 2007; 6: 85–94.
- [41] Li W, Zhang Z, Liu X, Cheng X, Zhang Y, Han X, et al. The FOXN3-NEAT1-SIN3A repressor complex promotes progression of hormonally responsive breast cancer. The Journal of Clinical Investigation. 2017; 127: 3421–3440.
- [42] Wang YG, Huang T, Wang JZ, Tang RX, Li S, Xiong Y. Mechanism of metformin inhibiting malignant cell phenotype of hepatocellular carcinoma cells through miR-194-5p/RBM6 pathway. Journal of Hebei Medical University. 2022; 43: 1371–1377, 1427. (In Chinese)
- [43] Li Z, Guo Q, Zhang J, Fu Z, Wang Y, Wang T, *et al.* The RNA-Binding Motif Protein Family in Cancer: Friend or Foe? Frontiers in Oncology. 2021; 11: 757135.
- [44] Hu J, Meng Y, Zeng J, Zeng B, Jiang X. Ubiquitin E3 Ligase MARCH7 promotes proliferation and invasion of cervical cancer cells through VAV2-RAC1-CDC42 pathway. Oncology Letters. 2018; 16: 2312–2318.
- [45] Shi D, Xie F, Zhang Y, Tian Y, Chen W, Fu L, et al. TFAP2A regulates nasopharyngeal carcinoma growth and survival by targeting HIF-1α signaling pathway. Cancer Prevention Research. 2014: 7: 266–277.
- [46] Berlato C, Chan KV, Price AM, Canosa M, Scibetta AG, Hurst HC. Alternative TFAP2A isoforms have distinct activities in breast cancer. Breast Cancer Research. 2011; 13: R23.
- [47] Tang H, Zeng L, Wang J, Zhang X, Ruan Q, Wang J, et al. Reversal of 5-fluorouracil resistance by EGCG is mediate by inactivation of TFAP2A/VEGF signaling pathway and down-regulation of MDR-1 and P-gp expression in gastric cancer. Oncotarget. 2017; 8: 82842–82853.
- [48] Pokrovskaja K, Panaretakis T, Grandér D. Alternative signaling pathways regulating type I interferon-induced apoptosis. Journal of Interferon & Cytokine Research. 2005; 25: 799–810.
- [49] Boukhaled GM, Harding S, Brooks DG. Opposing Roles of Type I Interferons in Cancer Immunity. Annual Review of Pathology. 2021; 16: 167–198.
- [50] Boehmer DFR, Formisano S, de Oliveira Mann CC, Mueller SA, Kluge M, Metzger P, et al. OAS1/RNase L executes RIG-I ligand-dependent tumor cell apoptosis. Science Immunology. 2021; 6: eabe2550.
- [51] Escher TE, Lui AJ, Geanes ES, Walter KR, Tawfik O, Hagan CR, et al. Interaction Between MUC1 and STAT1 Drives IFITM1 Overexpression in Aromatase Inhibitor-Resistant Breast Cancer Cells and Mediates Estrogen-Induced Apoptosis. Molecular Cancer Research. 2019; 17: 1180–1194.



- [52] Kim JC, Ha YJ, Tak KH, Roh SA, Kwon YH, Kim CW, et al. Opposite functions of GSN and OAS2 on colorectal cancer metastasis, mediating perineural and lymphovascular invasion, respectively. PLoS ONE. 2018; 13: e0202856.
- [53] L\u00e4 K, Li H, Wang S, Li A, Weng S, He J, et al. Interferon-Induced Protein 6-16 (IFI6-16) from *Litopenaeus vannamei* Regulate Antiviral Immunity via Apoptosis-Related Genes. Viruses. 2022; 14: 1062.
- [54] Ning S, Pagano JS, Barber GN. IRF7: activation, regulation, modification and function. Genes and Immunity. 2011; 12: 399– 414.
- [55] Wang Q, Chen P, Wang X, Wu Y, Xia K, Mu X, et al. piR-36249 and DHX36 together inhibit testicular cancer cells progression by upregulating OAS2. Non-Coding RNA Research. 2023; 8: 174–186.
- [56] Yoshida K, Miki Y. Role of BRCA1 and BRCA2 as regulators of DNA repair, transcription, and cell cycle in response to DNA damage. Cancer Science. 2004; 95: 866–871.
- [57] Liu J, Peng Y, Wei W. Cell cycle on the crossroad of tumorigenesis and cancer therapy. Trends in Cell Biology. 2022; 32: 30-44
- [58] Wang JY. DNA damage and apoptosis. Cell Death and Differentiation. 2001; 8: 1047–1048.
- [59] Pietrasik S, Zajac G, Morawiec J, Soszynski M, Fila M, Blasiak J. Interplay between BRCA1 and GADD45A and Its Potential for Nucleotide Excision Repair in Breast Cancer Pathogenesis. International Journal of Molecular Sciences. 2020; 21: 870.
- [60] Yoo S, Lee EJ, Thang NX, La H, Lee H, Park C, *et al.* INO80 Is Required for the Cell Cycle Control, Survival, and Differentiation of Mouse ESCs by Transcriptional Regulation. International Journal of Molecular Sciences. 2022; 23: 15402.
- [61] Lu Y, Zhang X. Radiochemotherapy-induced DNA repair promotes the biogenesis of gastric cancer stem cells. Stem Cell Re-

- search & Therapy. 2022; 13: 481.
- [62] Shi J, Lv X, Li W, Ming Z, Zeng L, Yuan J, et al. Overexpression of BCCIP predicts an unfavorable prognosis and promotes the proliferation and migration of lung adenocarcinoma. Thoracic Cancer. 2021; 12: 2324–2338.
- [63] Imbriano C, Molinari S. Alternative Splicing of Transcription Factors Genes in Muscle Physiology and Pathology. Genes. 2018; 9: 107.
- [64] Quereda V, Bayle S, Vena F, Frydman SM, Monastyrskyi A, Roush WR, et al. Therapeutic Targeting of CDK12/CDK13 in Triple-Negative Breast Cancer. Cancer Cell. 2019; 36: 545– 558.e7.
- [65] Diao B, Yang P. Comprehensive Analysis of the Expression and Prognosis for Laminin Genes in Ovarian Cancer. Pathology Oncology Research. 2021; 27: 1609855.
- [66] Gao E, Liu X, Yang Y, He Y, Xue D. OBSCN as biomarker for evaluating tumor mutation burden and anti-tumor immunity in Stomach adenocarcinoma. Research Square. 2022. (preprint)
- [67] Cui Y, Zhang C, Ma S, Guan F. TFAP2A-induced SLC2A1-AS1 promotes cancer cell proliferation. Biological Chemistry. 2021; 402: 717–727.
- [68] Feng Y, Qu L, Wang X, Liu C. LINC01133 promotes the progression of cervical cancer by sponging miR-4784 to up-regulate AHDC1. Cancer Biology & Therapy. 2019; 20: 1453–1461.
- [69] Lei T, Zhang W, He Y, Wei S, Song X, Zhu Y, et al. ZNF276 promotes the malignant phenotype of breast carcinoma by activating the CYP1B1-mediated Wnt/β-catenin pathway. Cell Death & Disease. 2022; 13: 781.
- [70] Wang H, Ji X. SMAD6, positively regulated by the DNM3OS-miR-134-5p axis, confers promoting effects to cell proliferation, migration and EMT process in retinoblastoma. Cancer Cell International. 2020; 20: 23.

